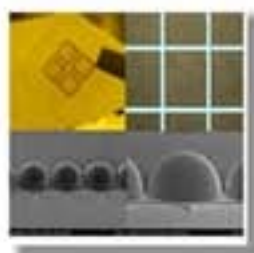


[Home](#)[Current Issue](#)[Issue in Progress](#)[Past Issues](#)[Early Posting](#)[About](#)[Editors & Staff](#)[Using Optics InfoBase](#)[Authors](#)[Reviewers](#)[Librarians](#)[Subscribe](#)[Optics InfoBase](#) > [Optics Letters](#) > [Volume 38](#) > [Issue 20](#) > Page 4182

Access brought to you by Korea University Library



Low-haze light extraction from organic light-emitting diode lighting with auxiliary electrode by selective microlens arrays

Ju Hyun Hwang, Tae Hyun Park, Hyun Jun Lee, Kyung Bok Choi, Young Wook Park, and Byeong-Kwon Ju [»View Author Affiliations](#)

Optics Letters, Vol. 38, Issue 20, pp. 4182-4185 (2013)
<http://dx.doi.org/10.1364/OL.38.004182>


View Full Text Article

[Enhanced HTML](#)[Acrobat PDF \(432 KB\)](#)[Abstract](#)[Article Info](#)[References \(14\)](#)[Cited By \(0\)](#)[Figures \(5\)](#)[Metrics](#)[Related Content](#)

Abstract

Improved out-coupling efficiency and low haze of organic light-emitting diode (OLED) lighting with an auxiliary electrode are demonstrated by selective microlens arrays (SMLAs). The microlens arrays, aligned with the auxiliary electrode, were selectively fabricated, since the fully packed microlens arrays lead to OLED lighting with high haze. The external quantum efficiency and power efficiency of the devices with the SMLAs increased by 32% when compared with the devices without these arrays. Using the SMLAs, dark grid lines in the emission region became brighter, with a low haze, and the spectra of the emitted light had no shift.

© 2013 Optical Society of America

[Journal Search](#)[Article Lookup](#)Optics Letters 

Search by title, abstract, or author


[Advanced Search](#)


Article Tools

Share



Citations

- Alert me when this article is cited
- Export Citation/Save 

Select an action... 

Low-haze light extraction from organic light-emitting diode lighting with auxiliary electrode by selective microlens arrays

Ju Hyun Hwang,¹ Tae Hyun Park,¹ Hyun Jun Lee,¹ Kyung Bok Choi,¹ Young Wook Park,^{2,3} and Byeong-Kwon Ju^{1,4}

¹Display and Nanosystem Laboratory, College of Engineering, Korea University, Seoul 136-713, South Korea

²The Institute of High Technology Materials and Devices, Korea University, Seoul 136-713, South Korea

³e-mail: zerook@korea.ac.kr

⁴e-mail: bkju@korea.ac.kr

Received August 27, 2013; accepted September 6, 2013;
posted September 12, 2013 (Doc. ID 196513); published October 11, 2013

Improved out-coupling efficiency and low haze of organic light-emitting diode (OLED) lighting with an auxiliary electrode are demonstrated by selective microlens arrays (SMLAs). The microlens arrays, aligned with the auxiliary electrode, were selectively fabricated, since the fully packed microlens arrays lead to OLED lighting with high haze. The external quantum efficiency and power efficiency of the devices with the SMLAs increased by 32% when compared with the devices without these arrays. Using the SMLAs, dark grid lines in the emission region became brighter, with a low haze, and the spectra of the emitted light had no shift. © 2013 Optical Society of America
OCIS codes: (230.3670) Light-emitting diodes; (250.0250) Optoelectronics.

<http://dx.doi.org/10.1364/OL.38.004182>

Organic light-emitting diodes (OLEDs) are attractive owing to their advantages of self-emission, low power consumption, high contrast ratios, high speed operation, ultrathin profile, and overall flexibility, and are applied in various fields such as flat panel displays and for illumination [1]. For practical white OLED (WOLED) lighting, electro-phosphorescence is widely used due to its 100% internal phosphorescence efficiency [2]. Additionally, the efficiency of the WOLEDs has been reported to exceed that of fluorescent tubes [3].

Although the internal quantum efficiency approaches 100%, significant research has been conducted on the light extraction techniques in OLEDs, because about 80% of light loss generated at the emission layer occurs in the indium-tin oxide (ITO)/organic mode, substrate mode, and surface plasmon mode [4]. The emitted light is trapped in the ITO/organic layer and glass substrate owing to the mismatch of the refractive indexes between the organic layers, ITO, glass substrate, and air. The ITO/organic mode has been out-coupled by a hexagonal-close-packed array [5], and ultra-low-index grid [6]. Additionally, the substrate mode has been extracted using microlens arrays [7,8] and zinc oxide pillar arrays [9].

In OLED lighting, the light out-coupling techniques mentioned above can be applied to extract the light in the ITO/organic mode. However, the haze is highly increased when applying extraction techniques to the glass substrate, such as microlens arrays and zinc oxide pillar arrays, which leave a regular pattern over the entire surface of the substrate so that OLED lighting becomes blurred and has a spectral shift [10].

As the size of the emissive area increases in OLED lighting, the nonuniformity of the emitted light is enhanced. The current in the large-area OLEDs mainly flows in the corner of the emission region. Thus the luminance at the center of the devices decreases, and the heat generation in the corner of the emission region increases [11,12]. An auxiliary metal electrode has been fabricated on the ITO to distribute holes onto the anode,

rendering the luminance and heat distribution uniform. Additionally, an insulator has been fabricated on the auxiliary electrode to avoid short circuits in the devices. However, the insulator on the auxiliary electrode blocks the hole injection from the auxiliary electrode into the organic layer. Furthermore, there is no recombination between the holes and electrons in the emissive area directly on the insulator, which reduces the effective emitting area [13].

In this study, selective microlens arrays (SMLAs), exactly aligned with the auxiliary metal electrode, are fabricated on the backside of the substrate to increase the external quantum efficiency and power efficiency, and to reduce the haze of OLED lighting. In the case of the microlens arrays fabricated on the entire surface of the glass substrate, the OLED lighting has blurred light and high haze along with a spectral shift, which is deleterious for OLED lighting. For these reasons, the fully packed microlens arrays on the glass substrate lead to OLED lighting with a high haze. Thus, the microlens arrays are selectively fabricated on the backside of the glass to extract light at the nonemissive area of the glass substrate under the insulator. Then, pure light can pass through the areas of the glass substrate, where the microlens arrays do not exist. As a result, the external quantum efficiency and power efficiency of the OLED lighting increase, and OLED lighting with low haze, is accomplished by the SMLAs. The SMLAs are fabricated by imprinting technology, which has a high reproducibility and can be applied to large-area OLEDs. The thickness, width, and arrangement of the SMLAs are simply controlled by spin-coating and photolithography. The SMLA has a high transmittance in the entire visible spectrum and has thermal and chemical resistances owing to the property of the SU-8 (SU-8 2025, MicroChem). Further, the refractive index of the resin is slightly higher than that of the glass substrate, which is appropriate for light extraction from the glass substrate into the SMLAs.

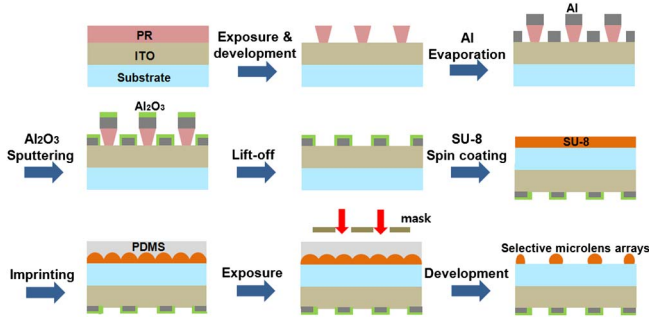


Fig. 1. Schematic illustration of fabrication procedures for the SMLAs and auxiliary electrode.

A schematic illustration of the fabrication procedures for the SMLA and auxiliary electrode is shown in Fig. 1. The negative tone photoresist AZ5214 was first spun on the ITO at a speed of 4000 rpm for 30 s, followed by a prebake at 95°C for 60 s. The AZ5214 was exposed to 25 mJ/cm² and annealed at 115°C for 2 min. After flood exposure without a mask, the AZ5214 was developed for 50 s. Thermal evaporation in high vacuum ($\sim 2 \times 10^{-6}$ Torr) was used to deposit an aluminum auxiliary electrode of 100 nm thickness. Al₂O₃ of 150 nm thickness was deposited onto the auxiliary electrode by radio frequency sputtering in order to fabricate an insulator. Then, the auxiliary electrode was fabricated under the insulator by a lift-off process.

For the fabrication of the microlens stamp, poly (dimethylsiloxane) (PDMS) elastomer was poured onto a microlens array (MNTECH Co. Ltd.) and cured in an oven at 70°C for over 3 h. The PDMS stamp could then be easily peeled off from the master, whose diameter was 78 μm and height was 53 μm. The height and width of the fabricated PDMS stamp were the same as those of the master. After fabricating the stamp, the photoresist SU-8 was spun onto the backside of the glass substrate, followed by annealing on a hotplate at 95°C for 6 min. Then, the substrate was completely cooled. The stamp and SU-8 were placed in contact at room temperature. A 1 kg iron block was placed on the combined stamp and SU-8, followed by heating in the oven at 100°C for 45 min. Next, the combined stamp and SU-8 were allowed to cool down. Afterward, the stamp was detached from the SU-8 [14]. Since the difference in the surface energies between the SU-8 and PDMS is small, the PDMS stamp was simply detached from the SU-8. Using an aligner and an optical microscope, UV light could be exposed to the SU-8 at the same position as the auxiliary electrode. After developing for 1 min in a sonicator (JAC-2010, Kodo Technical Research Co. Ltd.), followed by postbake at 160°C for 10 min, the SMLAs were completed.

The following layers were then thermally evaporated onto the auxiliary electrode and ITO of the anode in a high vacuum ($\sim 2 \times 10^{-6}$ Torr): a 60 nm thick N,N'-bis(a-naphthyl)-N,N'-diphenyl-1,1'-biphenyl-4,4'-diamine layer for hole transport, an 80 nm thick tris-(8-hydroxyquinoline) aluminum layer for light emission, a 0.8 nm thick lithium fluoride layer as an electron injection layer and 100 nm thick aluminum as a cathode layer.

Three types of devices were fabricated to study the effects of the SMLAs. All three device types have an

Table 1. Three Types of Fabricated Devices for Investigating the Effect of the SMLAs

Type	Structure of the Fabricated Devices
Device A	Glass/ITO/auxiliary electrode/NPB/Alq ₃ /LiF/Al
Device B	SMLAs with 78 μm width/glass/ITO/auxiliary electrode/NPB/Alq ₃ /LiF/Al
Device C	SMLAs with 312 μm width/glass/ITO/auxiliary electrode/NPB/Alq ₃ /LiF/Al

auxiliary electrode. Device A is a reference, without SMLAs; the other two devices comprise SMLAs with 78 and 312 μm widths, respectively (devices B and C). The device with 312 μm width SMLAs was composed of four SMLAs with a 78 μm width. The three types of fabricated devices are summarized in Table 1.

The current–voltage characteristics were measured using a Keithley 237 High-Voltage Source-Measure Unit (Keithley Instruments, Inc.), and the electroluminescence (EL) efficiency was measured using a Spectroradiometer (PR-670 SpectraScan, Photo Research, Inc.) in a dark box.

A photograph and optical microscope images of the auxiliary electrode with an insulator are shown in Figs. 2(a) and 2(b), and the scanning electron microscope (SEM) images of the SMLAs are represented in Figs. 2(c) and 2(d). The diameter and height of the SMLA are 82 and 45 μm, respectively, and the size ratio is appropriate for the light extraction, since the coupling enhancement factor of the microlens is highest at this ratio of hemisphere structure size. The height and width of the SMLAs are almost the same as those of the stamp. The stamp has a high reproducibility since the difference in the surface energies between the SU-8 and PDMS was small; therefore, there is no residue in the stamp after detachment. The SU-8 exhibits more than 95% transmittance in the visible light spectrum and has high thermal and chemical resistance. By controlling the exposure region in photolithography, devices B and C, with a height of 45 μm, were easily fabricated. In this fabrication technique, the shape of the arrangement is easily controlled by the mask patterns of the photolithography. Since the

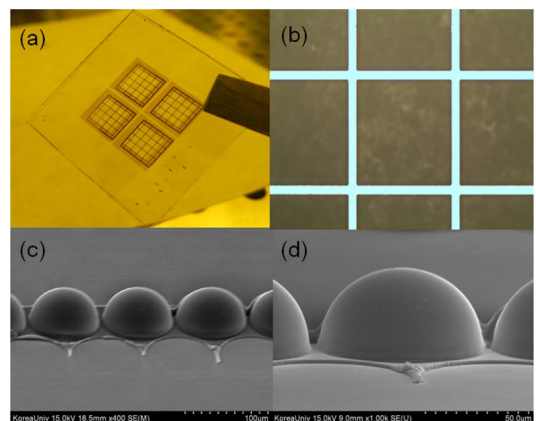


Fig. 2. (a) Photograph and (b) optical microscope image of the auxiliary electrode and insulator after the lift-off process. (c) and (d) Scanning electron microscope images of the SMLAs.

auxiliary electrode has a grid shape, the SMLAs also have an arrangement of grid patterns.

The EL characteristics of devices A–C are shown in Fig. 3. Figure 3(a) shows the current density as a function of voltage. The current densities of devices A–C are all similar in value because all these devices have the auxiliary electrode, which implies that the total resistance of

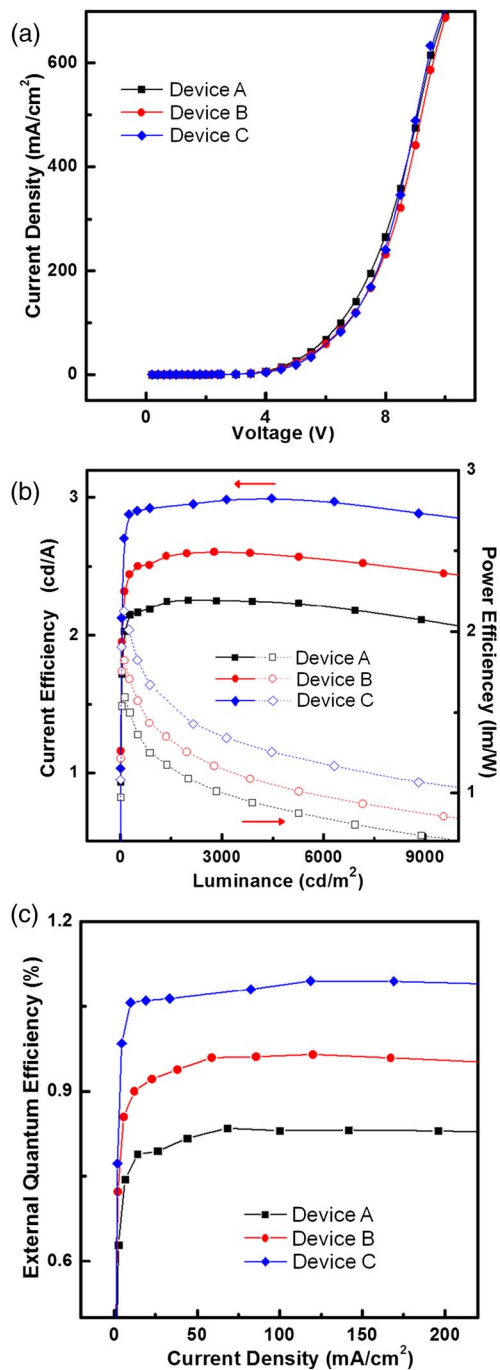


Fig. 3. (a) Current density–voltage characteristics. (b) Current efficiency and power efficiency as a function of luminance (solid and open symbols represent the current efficiency and power efficiency, respectively). (c) External quantum efficiency–current density characteristics of the OLEDs that have the auxiliary electrode without SMLAs (square), with 78 μm width SMLAs (circle), and with 312 μm width SMLAs (diamond).

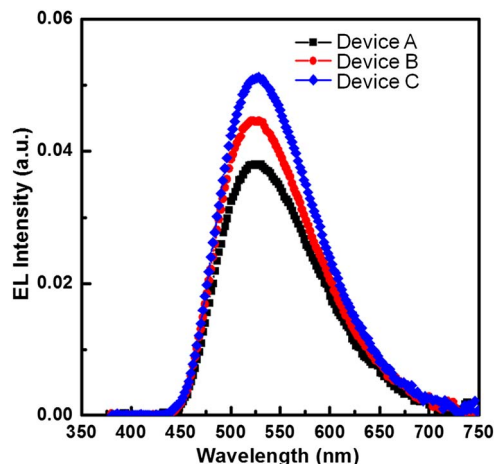


Fig. 4. Electroluminescence as a function of the wavelength of the OLEDs that have the auxiliary electrode without SMLAs (square), with 78 μm width SMLAs (circle), and with 312 μm width SMLAs (diamond), at a current density of 100 mA/cm^2 .

the devices is the same. The total resistance of the OLEDs with the auxiliary electrode is smaller than that of the OLEDs without the auxiliary electrode, which results in more current in the OLEDs with the auxiliary electrode. The device with wider SMLAs exhibits higher current efficiency and power efficiency, as shown in Fig. 3(b). The current efficiencies of the devices are 2.21 cd/A (device A), 2.52 cd/A (device B), and 2.92 cd/A (device C), respectively, at 1000 cd/m^2 , and their power efficiencies are: 1.12 lm/W (device A), 1.32 lm/W (device B), and 1.59 lm/W (device C), respectively, at 1000 cd/m^2 . These increases in the devices with SMLAs correspond to the enhancements of 17.8% (device B) and 41.9% (device C) in current efficiency, and 14.0% (device B), 32.1% (device C) in power efficiency.

The external quantum efficiency is plotted as a function of the current density in Fig. 3(c). The external quantum efficiency at 100 mA/cm^2 is 0.83% for device A, 0.96% for device B, and 1.09% for device C, respectively. The enhancement ratios correspond to 15.7% (device B) and 31.3% (device C) for the external quantum efficiency. The SU-8 of the SMLAs whose refractive index is approximately 1.57–1.63 at 380–780 nm is appropriate for light extraction, because the refractive index of the SU-8 is a little higher than that of the glass. When light passes from a material of low refractive index to a material of high refractive index, it changes its direction closer to the normal angle. At the SU-8/air interface, light passes with a low total reflection through the SMLA because of the hemispherical surface of the SMLA. The SMLAs aligned

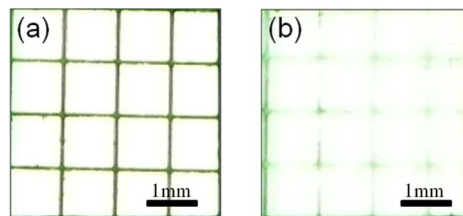


Fig. 5. Photographs of two types of OLEDs: (a) with only the auxiliary electrode (device A) and (b) with both the auxiliary electrode and SMLAs (device B).

Table 2. Haze and Total, Parallel, Diffuse Transmittance of the Four Types of Substrates

Type	Haze (%)	Total Transmittance (%)	Parallel Transmittance (%)	Diffuse Transmittance (%)
Ref	0.15	80.98	80.86	0.12
SMLAs 78	16.13	74.89	62.81	12.08
SMLAs 312	44.47	74.86	41.57	33.29
MLAs	76.94	79.66	18.37	61.29

with the auxiliary electrode extract the light totally reflected at the glass substrate/air interface and increase the efficiency of the devices with the auxiliary electrode. Consequently, the power efficiency and the external quantum efficiency are greatly enhanced, as the width of the SMLA increases owing to the increase in the light extraction area on the backside of the glass substrate.

Fig. 4 shows the EL spectra of the three devices at a current density of 100 mA/cm² in the visible light spectrum. The EL intensities of devices B and C are enhanced by 15.8% and 34.2%, respectively, at 525 nm. The peak intensity of the three devices in the EL spectrum is approximately 525 nm, and the total spectrum tendency of devices B and C is the same as that of device A, because the size of the SMLA is much larger than the emission wavelength.

As shown in Fig. 5, device A has black grid lines on the emissive area at an operating voltage 3.7 V and luminance of 60 cd/m². The insulator on the auxiliary electrode blocks the hole injection from the auxiliary electrode into the organic layer. As a result, there is no recombination between holes and electrons in the emissive area directly on the insulator, and light is not generated in the emissive layer on the insulator. Thus, the actual emission area of device A decreases, reducing the proportion in the emitting area by 11.4%. The width and length of the auxiliary electrode are 78 μm and 4 mm, respectively. Using the SMLAs, the dark grid lines in the emissive area of device B became brighter. The rest of the emissive area, where the microlens arrays do not exist, emitted pure light.

To investigate the haze of the SMLAs, four types of substrates were fabricated. A reference comprised of a 200 nm thick ITO on a 0.7 mm soda-lime glass (ITO glass). SMLAs 78, 312, and MLAs were composed of an ITO glass with 78 μm width SMLAs, 312 μm width SMLAs, and fully packed microlens arrays, respectively. The haze are 0.15% (Reference), 16.13% (SMLAs 78), 44.47% (SMLAs 312), and 76.94% (MLAs), respectively. As the total area of the microlens arrays on the ITO glass increases, the diffuse transmittance and haze also increase. Table 2 summarizes the haze and transmittances of each substrate.

In conclusion, we have fabricated SMLAs exactly aligned with the auxiliary electrode on the backside of a glass substrate. The totally reflected light at the glass substrate/air interface has been selectively extracted by the SMLAs. Therefore, the power efficiency and external quantum efficiency of the device increases, and the dark grid lines in the emission region become brighter, with low haze. As the total area of the SMLAs on the backside of the glass substrate increases, the haze as well as efficiency of the device increases. The efficiency and

haze are in a proportional relationship. Thus, depending on the goal of the efficiency and haze of the OLED lighting, the area of the SMLAs can be controlled.

Moreover, OLED lighting with the SMLAs exhibits no spectral shift. The SMLAs reduce the energy consumption of the OLED lightings by increasing the efficiency of the device. In terms of the fabrication process, the height, width, and arrangement of the SMLAs are simply controlled by spin-coating and photolithography. The imprinting technique used in the fabrication process has a high reproducibility and can be applied to large-area OLED lighting.

This research was supported by the Basic Science Research Program through the National Research Foundation of Korea (NRF) and funded by Korea government (MSIP) (CAFDC/Byeong-Kwon Ju/No. 2007-0056090), the NRF (No. 2012R1A6A3A04039396) Project of the MEST, the IT R&D program of MKE/KEIT (No. 2009-F-016-01, Development of Eco-Emotional OLED Flat-Panel Lighting, and the NRF Grant funded by the Korean Government (NRF-2012-Global Ph.D. Fellowship Program). The authors thank the staff of KBSI for technical assistance.

References

1. Y. Sun, N. C. Giebink, H. Kanno, B. Ma, M. E. Thompson, and S. R. Forrest, *Nature* **440**, 908 (2006).
2. C. Adachi, M. A. Baldo, M. E. Thompson, and S. R. Forrest, *J. Appl. Phys.* **90**, 5048 (2001).
3. S. Reineke, F. Lindner, G. Schwartz, N. Seidler, K. Walzer, B. Lüssem, and K. Leo, *Nature* **459**, 234 (2009).
4. B. C. Krummacher, S. Nowy, J. Frischeisen, M. Klein, and W. Brütting, *Org. Electron.* **10**, 478 (2009).
5. W. H. Koo, W. Youn, P. Zhu, X. H. Li, N. Tansu, and F. So, *Adv. Funct. Mater.* **22**, 3454 (2012).
6. M. Slightsky and S. R. Forrest, *Opt. Lett.* **35**, 1052 (2010).
7. S. H. Eom, E. Wrzesniewski, and J. Xue, *Org. Electron.* **12**, 472 (2011).
8. H. Y. Lin, Y. H. Ho, J. H. Lee, K. Y. Chen, J. H. Fang, S. C. Hsu, M. K. Wei, H. Y. Lin, J. H. Tsai, and T. C. Wu, *Opt. Express* **16**, 11044 (2008).
9. S. W. Liu, J. X. Wang, Y. Divayana, K. Dev, and S. T. Tan, *Appl. Phys. Lett.* **102**, 053305 (2013).
10. H. Y. Lin, J. H. Lee, M. K. Wei, K. Y. Chen, S. C. Hsu, Y. H. Ho, and C. Y. Lin, *Proc. SPIE* **6655**, 66551H (2007).
11. K. Neyts, M. Marescaux, A. U. Nieto, A. Elschner, and W. Lövenich, *J. Appl. Phys.* **100**, 114513 (2006).
12. J. W. Park, J. H. Lee, D. C. Shin, and S. H. Park, *J. Disp. Technol.* **5**, 306 (2009).
13. J. W. Park, D. C. Shin, and S. H. Park, *Semicond. Sci. Technol.* **26**, 034002 (2011).
14. X. Li, X. Wang, J. Jin, X. Li, Y. Tian, and S. Fu, *Proc. SPIE* **7657**, 76570Z (2010).